Journal of Nuclear Medicine, published on December 5, 2019 as doi:10.2967/jnumed.119.237198

Imaging P-glycoprotein Induction at the Blood-Brain Barrier of a Beta-Amyloidosis Mouse Model with ^{11}C-Metoclopramide PET

Viktoria Zoufal[1], Severin Mairinger[1], Mirjam Brackhan[2], Markus Krohn[2,†], Thomas Filip[1], Michael Sauberer[1], Johann Stanek[1], Thomas Wanek[1], Nicolas Tournier[3], Martin Bauer[4], Jens Pahnke[2,5,6,7], Oliver Langer[1,4,8,*]

[1]Preclinical Molecular Imaging, AIT Austrian Institute of Technology GmbH, Seibersdorf, Austria

[2]Department of Neuro-/Pathology, University of Oslo (UiO) and Oslo University Hospital (OUS), Oslo, Norway

[3]UMR 1023 IMIV, Service Hospitalier Frédéric Joliot, CEA, Inserm, Univ. Paris Sud, CNRS, Université Paris-Saclay, Orsay, France

[4]Department of Clinical Pharmacology, Medical University of Vienna, Vienna, Austria

[5]LIED, University of Lübeck, Germany

[6]Leibniz-Institute of Plant Biochemistry, Halle, Germany

[7]University of Latvia, Medical Faculty, Department of Pharmacology, Rīga, Latvia

[8]Department of Biomedical Imaging und Image-guided Therapy, Division of Nuclear Medicine, Medical University of Vienna, Vienna, Austria

[†]Current address: Institute for Experimental und Clinical Pharmacology and Toxicology, University of Lübeck, Lübeck, Germany

First author: Viktoria Zoufal (PhD student), Preclinical Molecular Imaging, AIT Austrian Institute of Technology GmbH, 2444 Seibersdorf, Austria; Email: viktoria.zoufal@chello.at

For correspondence contact: Oliver Langer, Preclinical Molecular Imaging, AIT Austrian Institute of Technology GmbH, 2444 Seibersdorf, Austria; ORCiD: 0000-0002-4048-5781; Email: oliver.langer@ait.ac.at

Short running foot line: Cerebral P-glycoprotein Induction

Financial support: This work was supported by the Austrian Science Fund (FWF) [I 1609-B24, to O. Langer], the Deutsche Forschungsgemeinschaft (DFG) [DFG PA930/9-1, to J. Pahnke] and the Lower Austria Corporation for Research and Education (NFB) [LS14-008, to T. Wanek].

Total word count: 5,220

ABSTRACT

P-glycoprotein (ABCB1) plays an important role at the blood-brain barrier (BBB) in promoting the clearance of neurotoxic beta-amyloid (Aβ) peptides from the brain into the blood. ABCB1 expression and activity were found to be decreased in the brains of Alzheimer disease (AD) patients. Treatment with drugs which induce cerebral ABCB1 activity may be a promising approach to delay the build-up of Aβ deposits in the brain by enhancing the clearance of Aβ peptides from the brain. The aim of this study was to investigate whether PET with the weak ABCB1 substrate radiotracer ^{11}C-metoclopramide can measure ABCB1 induction at the BBB in a beta-amyloidosis mouse model (APP/PS1-21 mice) and in wild-type mice.

Methods: Groups of wild-type and APP/PS1-21 mice aged 50 or 170 days underwent ^{11}C-metoclopramide baseline PET scans or scans after intraperitoneal treatment with the rodent pregnane X receptor (PXR) activator 5-pregnen-3β-ol-20-one-16α-carbonitrile (PCN, 25 mg/kg) or its vehicle over 7 days. At the end of the PET scans, brains were harvested for immunohistochemical analysis of ABCB1 and Aβ levels. In separate groups of mice, radiolabeled metabolites of ^{11}C-metoclopramide were determined in plasma and brain at 15 min after radiotracer injection. As an outcome parameter of cerebral ABCB1 activity, the elimination slope of radioactivity washout from the brain ($k_{E,brain}$) was calculated.

Results: PCN treatment resulted in an increased clearance of radioactivity from the brain as reflected by significant increases in $k_{E,brain}$ (from +26% to +54% relative to baseline). Immunohistochemical analysis confirmed ABCB1 induction in the brains of PCN-treated APP/PS1-21 mice with a concomitant decrease in Aβ levels. There was a significant positive correlation between $k_{E,brain}$ values and ABCB1 levels in the brain. In wild-type mice, a significant age-related decrease in $k_{E,brain}$ values was found. Metabolite analysis showed that the majority of radioactivity in the brain was composed of unmetabolized ^{11}C-metoclopramide in all animal

groups.

Conclusion: ^{11}C-metoclopramide can measure ABCB1 induction in the mouse brain without the need to consider an arterial input function and may find potential application in AD patients to non-invasively evaluate strategies to enhance the clearance properties of the BBB.

Key Words: Alzheimer disease; APP/PS1-21 mice; beta-amyloid clearance; P-glycoprotein induction; ^{11}C-metoclopramide

INTRODUCTION

A common feature of age-related neurodegenerative diseases (e.g. Alzheimer disease, Parkinson disease, frontotemporal dementia, Huntington disease and amyotrophic lateral sclerosis) is the presence of misfolded and aggregated proteins which lose their physiological roles and acquire neurotoxic properties (*1*). In these so-called proteinopathies, the accumulation of proteins in the brain has been linked to their insufficient clearance from the brain (*1-3*). Several different mechanisms for removal of neurotoxic proteins from the brain have been described, with the extrusion into the circulation *via* the blood-brain barrier (BBB) being an important mechanism (*1*). Transfer of substances across the BBB is tightly controlled. One important functional component of the BBB are adenosine triphosphate-binding cassette (ABC) transporters, which are mainly expressed in the luminal plasma membrane of brain capillary endothelial cells and which accept numerous endogenous and exogenous compounds as their substrates (*4*). An important representative of this family of transporters at the BBB is P-glycoprotein (ABC subfamily B member 1, ABCB1). ABCB1 was shown to work together with the low-density lipoprotein receptor-related protein 1 (LRP1) in the abluminal membrane of brain capillary endothelial cells in translocating beta-amyloid (Aβ) peptides across the BBB (*5*). Several studies found a decrease in ABCB1 expression and activity in patients and mouse models of Alzheimer disease (AD), which may contribute to a reduced Aβ clearance across the BBB (*6-10*).

Treatment with drugs which induce ABCB1 activity at the BBB may be a promising approach to attenuate AD symptoms caused by cerebral Aβ deposition by enhancing the clearance of neurotoxic Aβ peptides from the brain (*1*). Numerous signaling pathways which regulate cerebral ABC transporter expression are currently known (*11*). Agents targeting various components of these pathways have been tested in different beta-amyloidosis mouse models for their ability to restore ABCB1 activity/expression in the brain and thereby decrease cerebral

Aβ load (*9,12-14*). A future translation of such therapeutic approaches to AD patients critically depends on the availability of a diagnostic tool to measure ABCB1 activity at the human BBB.

PET with radiolabeled ABCB1 substrates, such as racemic ^{11}C-verapamil, (*R*)-^{11}C-verapamil and ^{11}C-*N*-desmethyl-loperamide, has shown great promise to study the effects of ABCB1 inhibition at the BBB on brain penetration of ABCB1 substrates (*15-17*). However, currently available PET tracers are avid substrates of ABCB1, which possess very low brain uptake when ABCB1 is fully functional, which limits their applicability to study the effects of ABCB1 induction at the BBB (*18,19*). Consequently, weak substrates of ABCB1 have been developed for PET, such as ^{11}C-metoclopramide (*20*) or ^{18}F-MC225 (*21*). Translational PET studies in rats, non-human primates and healthy human volunteers demonstrated that baseline brain uptake of ^{11}C-metoclopramide is substantially higher than that of (*R*)-^{11}C-verapamil or ^{11}C-*N*-desmethyl-loperamide and significantly increased following ABCB1 inhibition with tariquidar or cyclosporine A (*20,22,23*).

In the present study, we assessed the suitability of ^{11}C-metoclopramide to measure ABCB1 induction at the BBB in a commonly used beta-amyloidosis mouse model (APP/PS1-21 mice) (*24*) and in wild-type mice by employing a validated ABCB1 induction protocol based on treatment with the prototypical rodent pregnane X receptor (PXR) activator 5-pregnen-3β-ol-20-one-16α-carbonitrile (PCN) (*9*).

MATERIALS AND METHODS

Chemicals

Unless otherwise stated, all chemicals were purchased from Sigma-Aldrich (Schnelldorf, Germany) or Merck (Darmstadt, Germany). Metoclopramide ampoules (Paspertin®, 10 mg/2 mL) were obtained from a local pharmacy. PCN was dissolved in safflower oil containing 5% (v/v) dimethyl sulfoxide and was injected intraperitoneally (i.p.) into mice at a dose of 25 mg/kg body weight (*9*).

Radiotracer Synthesis

^{11}C-metoclopramide was synthesized as described before (*25*). For intravenous (i.v.) injection into animals, ^{11}C-metoclopramide was formulated in 0.9% (w/v) physiological saline and 10 µL Paspertin® solution (containing 0.05 mg of unlabeled metoclopramide) was added to each injected dose (to slow down peripheral metabolism of the radiotracer) (*20*). Radiochemical purity was >98%.

Animals

Female transgenic mice, which express mutated human amyloid precursor protein (APP) and presenilin 1 (PS1) under control of the Thy1-promoter ($APP_{KM670/671NL}$, PS_{L166P}) (referred to as APP/PS1-21 mice) (*24*) and wild-type mice were maintained in a C57BL/6J genetic background at the University of Oslo. Two different age groups of wild-type mice were examined: approximately 50 days (mean age: 48±1 days, mean weight: 18.9±1.9 g) and approximately 170 days (mean age: 162±26 days, mean weight: 26.8±3.5 g). APP/PS1-21 mice were investigated at an approximate age of 50 days (mean age: 52±1 days, mean weight: 18.4±1.3 g) and 170 days (mean age: 168±20 days, mean weight: 24.6±2.3 g). In total, 65 mice were used in the experiments.

The study was approved by the national authorities (Amt der Niederösterreichischen Landesregierung) and study procedures were in accordance with the European Communities Council Directive of September 22, 2010 (2010/63/EU). The animal experimental data reported in this study are in compliance with the ARRIVE (Animal Research: Reporting in Vivo Experiments) guidelines.

Experimental Design

An overview of examined animal groups is given in Table 1. Groups of wild-type and APP/PS1-21 mice underwent a baseline PET scan with ^{11}C-metoclopramide. After the baseline scan, animals were i.p. treated for 7 days once daily with PCN (25 mg/kg) or with vehicle solution (5% dimethyl sulfoxide in safflower oil). In case of APP/PS1-21 mice, a separate group of animals (which had not undergone baseline PET scans) was used for PCN treatment (to improve tolerability of PCN treatment). On the day following the last treatment, animals underwent a PET scan with ^{11}C-metoclopramide. The dosage of PCN was selected based on previous work (*9*). Separate groups of vehicle- and PCN-treated animals were used to assess radiotracer metabolism (see below).

PET Imaging

Imaging experiments were performed under isoflurane/air anesthesia. Animals were warmed throughout the experiment and body temperature and respiratory rate were constantly monitored. Mice were placed in a custom-made imaging chamber and a lateral tail vein was cannulated. A microPET Focus220 scanner (Siemens Medical Solutions, Knoxville, TN, USA) was used for PET imaging. ^{11}C-metoclopramide (26±6 MBq in a volume of 100 µL) was administered as an i.v. bolus over 60 sec and a 90-min dynamic PET scan was initiated at the start of radiotracer injection. List-mode data were acquired with a timing window of 6 ns and an energy

window of 250-750 keV. After the 7-day treatment period, mice underwent a 90-min dynamic ^{11}C-metoclopramide PET scan using the same acquisition parameters. At the end of the PET scan, a blood sample was collected from the retro-bulbar plexus and animals were killed by cervical dislocation. Blood was centrifuged to obtain plasma, and aliquots of blood and plasma were measured for radioactivity in a gamma counter. Whole brains were removed, incubated in 30% sucrose solution and embedded in Tissue Freezing Medium (Tissue-Tek® O.C.T™ Compound, Sakura Finetek). Samples were snap frozen in liquid nitrogen and stored at -80°C for immunohistochemistry of ABCB1 and Aβ as described in the Supplemental Materials and Methods.

Metabolism

In separate groups of wild-type and APP/PS1-21 mice, plasma and brain samples were analyzed with radio-thin-layer chromatography for radiolabeled metabolites of ^{11}C-metoclopramide at 15 min after radiotracer injection as described in the Supplemental Materials and Methods.

PET Data Analysis

The PET data were sorted into 25 time frames with a duration increasing from 5 sec to 20 min. PET images were reconstructed using Fourier re-binning of the 3-dimensional sinograms followed by a 2-dimensional filtered back-projection with a ramp filter giving a voxel size of 0.4 x 0.4 x 0.796 mm³. Using PMOD software (version 3.6, PMOD Technologies Ltd., Zurich, Switzerland), hippocampus, cortex and cerebellum were outlined on the PET images using the Mirrione Mouse Atlas and guided by representative magnetic resonance (MR) images obtained in a few animals on a 1 Tesla benchtop MR scanner (ICON, Bruker BioSpin GmbH, Ettlingen,

Germany). Regions of interest were manually adjusted if necessary to derive time-activity curves (TACs) expressed in units of standardized uptake value (SUV) ((radioactivity per g/injected radioactivity) x body weight). From the log-transformed TACs in hippocampus, cortex and cerebellum the elimination slope of radioactivity washout ($k_{E,brain}$, 1/h) was determined by linear regression analysis of data from 17.5 to 80 min after radiotracer injection (which best reflected the linear elimination phase in the log-transformed TACs) (*22,23*).

Statistical Analysis

Statistical testing was performed using Prism 8.0 software (GraphPad, La Jolla, CA, USA). Differences between multiple groups were analyzed by one-way ANOVA followed by a Tukey's multiple comparison test and differences between two groups were analyzed by a 2-sided unpaired *t*-test. Pearson correlation coefficient (*r)* was calculated to assess correlations. The level of statistical significance was set to $P<0.05$. All values are given as mean ± standard deviation (SD).

RESULTS

We used ^{11}C-metoclopramide PET to measure cerebral ABCB1 activity in groups of wild-type and APP/PS1-21 mice at baseline and after treatment with the ABCB1 inducer PCN (25 mg/kg) or its vehicle over 7 days. In Table 1, an overview of all examined mouse groups and corresponding animal numbers is given. Out of a total number of 65 animals, 20 animals died either during the treatment periods (8 animals) or during anesthesia (12 animals). PCN treatment resulted in 4 and 3 animal losses in the wild-type and APP/PS1-21 groups, respectively (PET and metabolism).

Neither treatment with PCN nor its vehicle led to significant changes in total radioactivity concentrations in blood or plasma measured at the end of the PET scan (Supplemental Fig. 1). Analysis of radiolabeled metabolites of ^{11}C-metoclopramide at 15 min after radiotracer injection showed that approximately 60-75% of total radioactivity in plasma was composed of unidentified polar radiolabeled metabolites, while the majority (>80%) of radioactivity in the brain was composed of unmetabolized ^{11}C-metoclopramide (Supplemental Table 1). There was no significant difference in the percentage of unmetabolized ^{11}C-metoclopramide in the brain between PCN-treated mice and vehicle-treated wild-type or APP/PS1-21 mice. In plasma, the percentage of unmetabolized ^{11}C-metoclopramide was significantly lower in PCN-treated mice than in vehicle-treated wild-type mice.

In Figure 1, coronal ^{11}C-metoclopramide PET summation images of wild-type and APP/PS1-21 mice at baseline and after treatment with PCN or vehicle are shown. For both mouse strains, PCN-treated animals had visually lower brain radioactivity concentrations. We outlined hippocampus and cortex as brain regions with substantial Aβ deposition and cerebellum as a control region with minimal Aβ deposition (Supplemental Fig. 2). In Figure 2, the TACs for these

regions are shown. In all three examined regions, PCN-treated wild-type and APP/PS1-21 mice showed a markedly increased washout of radioactivity as compared with the other groups (Fig. 2).

Brain slices of PCN- and vehicle-treated APP/PS1-21 mice were immunohistochemically stained for ABCB1 and Aβ (Supplemental Fig. 3). A semi-quantitative analysis of the stained microvessels indicated significantly increased ABCB1 levels in the hippocampus, cortex and cerebellum of PCN-treated compared to vehicle-treated APP/PS1-21 mice (Fig. 3A). In addition, a significant reduction in Aβ plaque load was observed in the hippocampus and cortex of PCN-treated mice (Fig. 3A). There was a significant negative correlation between Aβ plaque load and ABCB1 levels in the hippocampus and a trend towards a negative correlation in the cortex (Fig. 3B). In the cerebellum, this correlation could not be assessed due to absence of Aβ plaques.

As an outcome parameter of cerebral ABCB1 activity, we determined the elimination slope of radioactivity washout from the brain from 17.5 to 80 min after radiotracer injection ($k_{E,brain}$) as described previously (*22,23*). Mean $k_{E,brain}$ values in all studied animal groups are given in Supplemental Table 2. $k_{E,brain}$ was significantly increased in all three brain regions of PCN-treated wild-type and APP/PS1-21 mice (from +26% to +54% relative to respective baseline group) (Fig. 4). There was a significant positive correlation between $k_{E,brain}$ and ABCB1 levels in the cortex and cerebellum of APP/PS1-21 mice and a trend towards a positive correlation in the hippocampus (Fig. 5).

We also performed baseline ^{11}C-metoclopramide PET scans in 50-days old wild-type and APP/PS1-21 mice to study possible age-related differences in cerebral ABCB1 activity. In all three brain regions of wild-type mice, there was a significant age-related decrease in $k_{E,brain}$ values (from -10% to -26%), while this effect was not observed in APP/PS1-21 mice (Fig. 6). $k_{E,brain}$ did not differ significantly in any studied brain region between age-matched wild-type and APP/PS1-21 mice.

DISCUSSION

The aim of this study was to investigate whether the weak ABCB1 substrate radiotracer ^{11}C-metoclopramide can measure ABCB1 induction at the mouse BBB. We found that treatment of wild-type and APP/PS1-21 mice with the prototypical rodent PXR ligand PCN led to significant increases in the brain clearance of ^{11}C-metoclopramide, which was consistent with ABCB1 induction. Moreover, the outcome parameter of ^{11}C-metoclopramide elimination from the brain ($k_{E,brain}$) was shown to be correlated with cerebral ABCB1 levels, which supported the ability of ^{11}C-metoclopramide to measure ABCB1 activity in the mouse brain and highlighted the potential of ^{11}C-metoclopramide for future clinical translation to measure ABCB1 induction at the human BBB.

Currently available PET tracers for ABCB1 (^{11}C-verapamil, (*R*)-^{11}C-verapamil and ^{11}C-*N*-desmethyl-loperamide) are very efficiently transported by ABCB1 at the BBB, which results in very low brain uptake and a limited sensitivity to measure moderate changes in ABCB1 activity at the BBB (*18,19*). Moreover, (*R*)-^{11}C-verapamil is extensively metabolized in humans, which gives rise to radiolabeled metabolites, which may be able to penetrate the BBB and thereby confound the measurement of ABCB1 activity (*26*). One study has so far attempted to measure ABCB1 induction at the human BBB with ^{11}C-verapamil PET following treatment of healthy volunteers with the PXR activator rifampicin (*27*). This study failed to demonstrate an effect of rifampicin on cerebral ABCB1 activity, which may either be attributed to the inability of rifampicin to induce ABCB1 at the human BBB or the lack of sensitivity of ^{11}C-verapamil to measure ABCB1 induction.

^{11}C-metoclopramide was found to be *in vitro* a substrate of human ABCB1, while not being transported by breast cancer resistance protein (ABCG2), another major ABC transporter at the BBB (*20*). Moreover, chromatographic analysis of brain tissue homogenates obtained after i.v. injection of ^{11}C-metoclopramide into rats demonstrated an absence of radiolabeled metabolites,

suggesting that measurement of cerebral ABCB1 activity is not confounded by brain-penetrant radiolabeled metabolites (*20*). Finally, as opposed to avid ABCB1 substrates, pharmacological inhibition of ABCB1 at the BBB was shown to mainly decrease the efflux rate constant of ^{11}C-metoclopramide from the brain into the blood (k_2), rather than increase the influx rate constant from plasma into the brain (K_1) (*19*). As the estimation of k_2 requires a metabolite-corrected arterial input function, $k_{E,brain}$ has been proposed as a parameter reflecting cerebral ABCB1 activity, which can be directly derived from the brain TACs without the need to consider an arterial input function (*22,23*). A significant decrease in $k_{E,brain}$ was found in non-human primates and healthy human volunteers following ABCB1 inhibition with tariquidar or cyclosporine A (*22,23*). Considering that the performance of continuous arterial blood sampling is very challenging in mice, $k_{E,brain}$ was employed in the present study as an outcome parameter of cerebral ABCB1 activity. We co-injected ^{11}C-metoclopramide with unlabeled metoclopramide (2 mg/kg), because a previous study in rats had shown that this slows down the peripheral metabolism of the radiotracer while maintaining the ability of the radiotracer to measure cerebral ABCB1 activity (*20*). Nevertheless, substantial metabolism of ^{11}C-metoclopramide was observed with only 25-40% of total radioactivity in plasma being in the form of unmetabolized radiotracer at 15 min after radiotracer injection (Supplemental Table 1). Importantly, in accordance with previous data in rats (*20*), we could demonstrate that most of the radioactivity in the mouse brain was composed of unmetabolized ^{11}C-metoclopramide. The fast plasma clearance of ^{11}C-metoclopramide in mice may be of advantage to employ $k_{E,brain}$ as a parameter of cerebral ABCB1 activity, as it suggests that $k_{E,brain}$ will approximate the clearance of ^{11}C-metoclopramide from brain into blood. However, this would require validation by performing arterial blood sampling and kinetic modeling to compare modeling-derived k_2 values with $k_{E,brain}$.

We employed a validated treatment protocol with the rodent PXR activator PCN to induce ABCB1 expression at the mouse BBB (*9*). PXR is a nuclear receptor which regulates the expression of metabolic enzymes and transporters involved in the clearance of xenobiotics from the body. Hartz et al. have shown an increase in ABCB1 expression and activity and a concomitant decrease in Aβ levels in isolated brain microvessels of 12-weeks old Tg2576 mice treated i.p. over 7 days with PCN (25 mg/kg) as compared with vehicle-treated animals (*9*). These previous findings could be confirmed in our study, in which the same PCN treatment protocol led to significant increases in ABCB1 levels in all studied brain regions of APP/PS1-21 mice (Fig. 3). Moreover, a significant reduction in hippocampal and cortical Aβ levels was observed in PCN-treated mice as well as a negative correlation between Aβ and ABCB1 levels. A similar inverse correlation between Aβ and ABCB1 has been reported in brain tissue of non-demented elderly subjects (*28*). PCN treatment increased the percentage of radiolabeled metabolites of ^{11}C-metoclopramide in plasma, which was consistent with the known CYP450 enzyme-inducing effect of PXR activation in the liver, but this had no effect on the composition of radioactivity in the brain (Supplemental Table 1). Baseline brain uptake of ^{11}C-metoclopramide was higher than described previously in the same mouse strain for the avid ABCB1 substrates (*R*)-^{11}C-verapamil and ^{11}C-*N*-desmethyl-loperamide (*29*). Both in wild-type and APP-PS1-21 mice, PCN treatment accelerated the washout of radioactivity from the brain as reflected by a significant increase in the $k_{E,brain}$ parameter (Figs. 2 and 4). Moreover, $k_{E,brain}$ values in individual animals showed a positive correlation with the respective cerebral ABCB1 levels (Fig. 5), which corroborated the use of $k_{E,brain}$ as an outcome parameter for non-invasive determination of cerebral ABCB1 activity.

Accumulating evidence points to an age-related decline in cerebral ABCB1 expression and activity (*30*). In line with this, $k_{E,brain}$ values were found to be significantly lower in all three brain regions of 170-days old wild-type mice as compared with the 50-days old age group (Fig. 6).

However, no statistically significant age-related decrease in $k_{E,brain}$ values was found in APP/PS1-21 mice. Moreover, no differences in $k_{E,brain}$ values were detected between age-matched wild-type and APP/PS1-21 mice. This is surprising given the fact that we have previously found significantly reduced hippocampal and cortical ABCB1 levels in 200-days old APP/PS1-21 mice as compared with age-matched wild-type mice (*6*). This could indicate that additional alterations may have occurred at the BBB of APP/PS1-21 mice (e.g. decreases in cerebral blood flow, changes in structure/composition of the basement membrane) (*7*), which could have masked the impact of reduced ABCB1 expression on the brain kinetics of ^{11}C-metoclopramide. A possible alternative explanation could be that the lot of wild-type and APP/PS1-21 mice used in the present study - even though it was obtained from the same source as in our previous study (*6*) - showed no differences in cerebral ABCB1 levels, which could not be confirmed due to a lack of immunohistochemical data for wild-type mice.

CONCLUSION

Our data provide clear evidence for the suitability of ^{11}C-metoclopramide, a novel weak ABCB1 substrate radiotracer, to measure ABCB1 induction at the mouse BBB without the need to consider an arterial input function. ^{11}C-metoclopramide may overcome the limitations of previously described avid ABCB1 substrate radiotracers and provide an imaging-based biomarker for the development of novel ABCB1-inducing AD therapeutics. Next to measuring pharmacological induction of cerebral ABCB1, ^{11}C-metoclopramide PET may also be suitable to measure a disease-induced increase in cerebral ABCB1 activity (e.g. in drug-resistant epilepsy).

DISCLOSURE

This work was supported by the Austrian Science Fund (FWF) [I 1609-B24, to O. Langer], the Deutsche Forschungsgemeinschaft (DFG) [DFG PA930/9-1, to J. Pahnke] and the Lower Austria Corporation for Research and Education (NFB) [LS14-008, to T. Wanek]. The work of J. Pahnke was further supported by the following grants: Deutsche Forschungsgemeinschaft/Germany [DFG PA930/12], Wirtschaftsministerium Sachen-Anhalt [EFRE, ZS/2016/05/78617], the Leibniz Association [Leibniz-Wettbewerb SAW-2015-IPB-2], Latvian Council of Science FLPP/Latvia [lzp-2018/1-0275], Nasjonalforeningen [16154], HelseSØ/Norway [2016062, 2019054, 2019055], Norsk forskningsrådet/Norway [251290 FRIMEDIO, 260786 PROP-AD] and Horizon 2020/European Union [643417, PROP-AD]. PROP-AD is an EU Joint Programme-Neurodegenerative Disease Research (JPND) project. The project is supported through the following funding organizations under the aegis of JPND-www.jpnd.eu: AKA #301228-Finland, BMBF #01ED1605-Germany, CSO-MOH #30000-12631-Israel, NFR #260786-Norway, SRC #2015-06795-Sweden. This project has received funding from the European Union's Horizon 2020 research and innovation programme under grant agreement #643417 (JPco-fuND). No other potential conflicts of interest relevant to this article exist.

ACKNOWLEDGMENTS

The authors wish to thank Mathilde Löbsch for help in conducting the PET experiments.

KEY POINTS

Question: Can ^{11}C-metoclopramide PET measure ABCB1 induction at the BBB?

Pertinent Findings: Treatment of wild-type and APP/PS1-21 mice with the prototypical rodent PXR activator PCN over 7 days led to a significant increase in the washout of ^{11}C-metoclopramide

from the brain ($k_{E,brain}$). Immunohistochemical analysis confirmed ABCB1 induction in PCN-treated APP/PS1-21 mice and a concomitant reduction in Aβ load.

Implications for Patient Care: ^{11}C-metoclopramide PET may aid in the future development of novel therapeutics for the treatment of AD, which increase cerebral ABCB1 activity to enhance clearance of neurotoxic Aβ peptides from the brain.

REFERENCES

1. Boland B, Yu WH, Corti O, et al. Promoting the clearance of neurotoxic proteins in neurodegenerative disorders of ageing. *Nat Rev Drug Discov.* 2018;17:660-688.
2. Mawuenyega KG, Sigurdson W, Ovod V, et al. Decreased clearance of CNS beta-amyloid in Alzheimer's disease. *Science.* 2010;330:1774.
3. Hardy J, Allsop D. Amyloid deposition as the central event in the aetiology of Alzheimer's disease. *Trends Pharmacol Sci.* 1991;12:383-388.
4. Abbott NJ, Patabendige AA, Dolman DE, Yusof SR, Begley DJ. Structure and function of the blood-brain barrier. *Neurobiol Dis.* 2010;37:13-25.
5. Storck SE, Hartz AMS, Bernard J, et al. The concerted amyloid-beta clearance of LRP1 and ABCB1/P-gp across the blood-brain barrier is linked by PICALM. *Brain Behav Immun.* 2018;73:21-33.
6. Zoufal V, Wanek T, Krohn M, et al. Age dependency of cerebral P-glycoprotein function in wild-type and APPPS1 mice measured with PET. *J Cereb Blood Flow Metab.* October 24, 2018 [Epub ahead of print].
7. Mehta DC, Short JL, Nicolazzo JA. Altered brain uptake of therapeutics in a triple transgenic mouse model of Alzheimer's disease. *Pharm Res.* 2013;30:2868-2879.
8. Kannan P, Schain M, Kretzschmar WW, et al. An automated method measures variability in P-glycoprotein and ABCG2 densities across brain regions and brain matter. *J Cereb Blood Flow Metab.* 2017;37:2062-2075.
9. Hartz AM, Miller DS, Bauer B. Restoring blood-brain barrier P-glycoprotein reduces brain amyloid-beta in a mouse model of Alzheimer's disease. *Mol Pharmacol.* 2010;77:715-723.

10. Deo AK, Borson S, Link JM, et al. Activity of P-glycoprotein, a beta-amyloid transporter at the blood-brain barrier, is compromised in patients with mild Alzheimer disease. *J Nucl Med.* 2014;55:1106-1111.

11. Miller DS. Regulation of ABC transporters blood-brain barrier: the good, the bad, and the ugly. *Adv Cancer Res.* 2015;125:43-70.

12. Qosa H, Abuznait AH, Hill RA, Kaddoumi A. Enhanced brain amyloid-beta clearance by rifampicin and caffeine as a possible protective mechanism against Alzheimer's disease. *J Alzheimers Dis.* 2012;31:151-165.

13. Brenn A, Grube M, Jedlitschky G, et al. St. John's Wort reduces beta-amyloid accumulation in a double transgenic Alzheimer's disease mouse model-role of P-glycoprotein. *Brain Pathol.* 2014;24:18-24.

14. Durk MR, Han K, Chow EC, et al. 1alpha,25-Dihydroxyvitamin D3 reduces cerebral amyloid-beta accumulation and improves cognition in mouse models of Alzheimer's disease. *J Neurosci.* 2014;34:7091-7101.

15. Muzi M, Mankoff DA, Link JM, et al. Imaging of cyclosporine inhibition of P-glycoprotein activity using ^{11}C-verapamil in the brain: studies of healthy humans. *J Nucl Med.* 2009;50:1267-1275.

16. Kreisl WC, Bhatia R, Morse CL, et al. Increased permeability-glycoprotein inhibition at the human blood-brain barrier can be safely achieved by performing PET during peak plasma concentrations of tariquidar. *J Nucl Med.* 2015;56:82-87.

17. Bauer M, Karch R, Zeitlinger M, et al. Approaching complete inhibition of P-glycoprotein at the human blood-brain barrier: an (*R*)-[^{11}C]verapamil PET study. *J Cereb Blood Flow Metab.* 2015;35:743-746.

18. Tournier N, Stieger B, Langer O. Imaging techniques to study drug transporter function in vivo. *Pharmacol Ther.* 2018;189:104-122.

19. Bauer M, Tournier N, Langer O. Imaging P-glycoprotein function at the blood-brain barrier as a determinant of the variability in response to central nervous system drugs. *Clin Pharmacol Ther.* 2019;105:1061-1064.

20. Pottier G, Marie S, Goutal S, et al. Imaging the impact of the P-glycoprotein (ABCB1) function on the brain kinetics of metoclopramide. *J Nucl Med.* 2016;57:309-314.

21. Savolainen H, Windhorst AD, Elsinga PH, et al. Evaluation of [^{18}F]MC225 as a PET radiotracer for measuring P-glycoprotein function at the blood-brain barrier in rats: Kinetics, metabolism, and selectivity. *J Cereb Blood Flow Metab.* 2017;37:1286-1298.

22. Tournier N, Bauer M, Pichler V, et al. Impact of P-glycoprotein function on the brain kinetics of the weak substrate ^{11}C-metoclopramide assessed with PET imaging in humans. *J Nucl Med.* 2019;60:985-991.

23. Auvity S, Caillé F, Marie S, et al. P-glycoprotein (ABCB1) inhibits the influx and increases the efflux of ^{11}C-metoclopramide across the blood-brain barrier: a PET study on non-human primates. *J Nucl Med.* 2018;59:1609-1615.

24. Radde R, Bolmont T, Kaeser SA, et al. Abeta42-driven cerebral amyloidosis in transgenic mice reveals early and robust pathology. *EMBO Rep.* 2006;7:940-946.

25. Caillé F, Goutal S, Marie S, et al. Positron emission tomography imaging reveals an importance of saturable liver uptake transport for the pharmacokinetics of metoclopramide. *Contrast Media Mol Imaging.* 2018;2018:7310146.

26. Luurtsema G, Molthoff CF, Schuit RC, Windhorst AD, Lammertsma AA, Franssen EJ. Evaluation of (*R*)-[^{11}C]verapamil as PET tracer of P-glycoprotein function in the blood-brain barrier: kinetics and metabolism in the rat. *Nucl Med Biol.* 2005;32:87-93.

27. Liu L, Collier AC, Link JM, et al. Modulation of P-glycoprotein at the human blood-brain barrier by quinidine or rifampin treatment: a PET imaging study. *Drug Metab Dispos.* 2015;43:1795-1804.

28. Vogelgesang S, Cascorbi I, Schroeder E, et al. Deposition of Alzheimer's beta-amyloid is inversely correlated with P-glycoprotein expression in the brains of elderly non-demented humans. *Pharmacogenetics.* 2002;12:535-541.

29. Wanek T, Römermann K, Mairinger S, et al. Factors governing p-glycoprotein-mediated drug-drug interactions at the blood-brain barrier measured with positron emission tomography. *Mol Pharm.* 2015;12:3214-3225.

30. Pan Y, Nicolazzo JA. Impact of aging, Alzheimer's disease and Parkinson's disease on the blood-brain barrier transport of therapeutics. *Adv Drug Deliv Rev.* 2018;135:62-74.

TABLE 1

Overview of Examined Animal Groups and Numbers

	PET		Metabolism
	Age (days)		Age (days)
Group	50 d	170 d	170 d
Wild-type baseline	5	10	0
Wild-type PCN	0	4*	1
Wild-type vehicle	0	3*	3
APP/PS1-21 baseline	8	6	0
APP/PS1-21 PCN	0	8	2
APP/PS1-21 vehicle	0	4*	4

*Same animals also received a baseline scan.

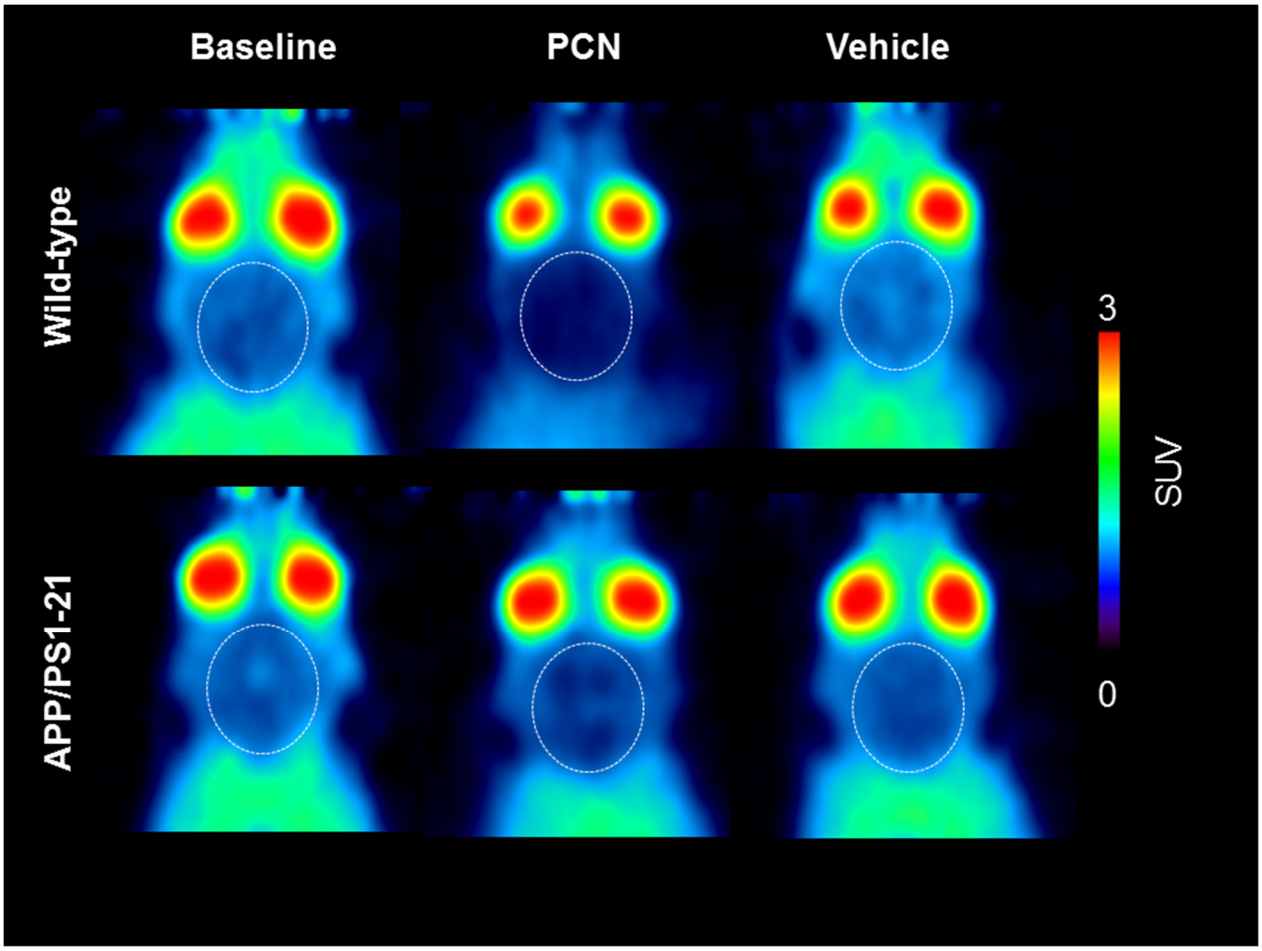

FIGURE 1. Coronal PET summation images (17.5-80 min) of wild-type and APP/PS1-21 mice aged 170 days for baseline scan and scan after i.p. treatment with PCN or vehicle. Whole brain region is highlighted with a white broken line. All images are set to the same intensity scale (0-3 standardized uptake value, SUV).

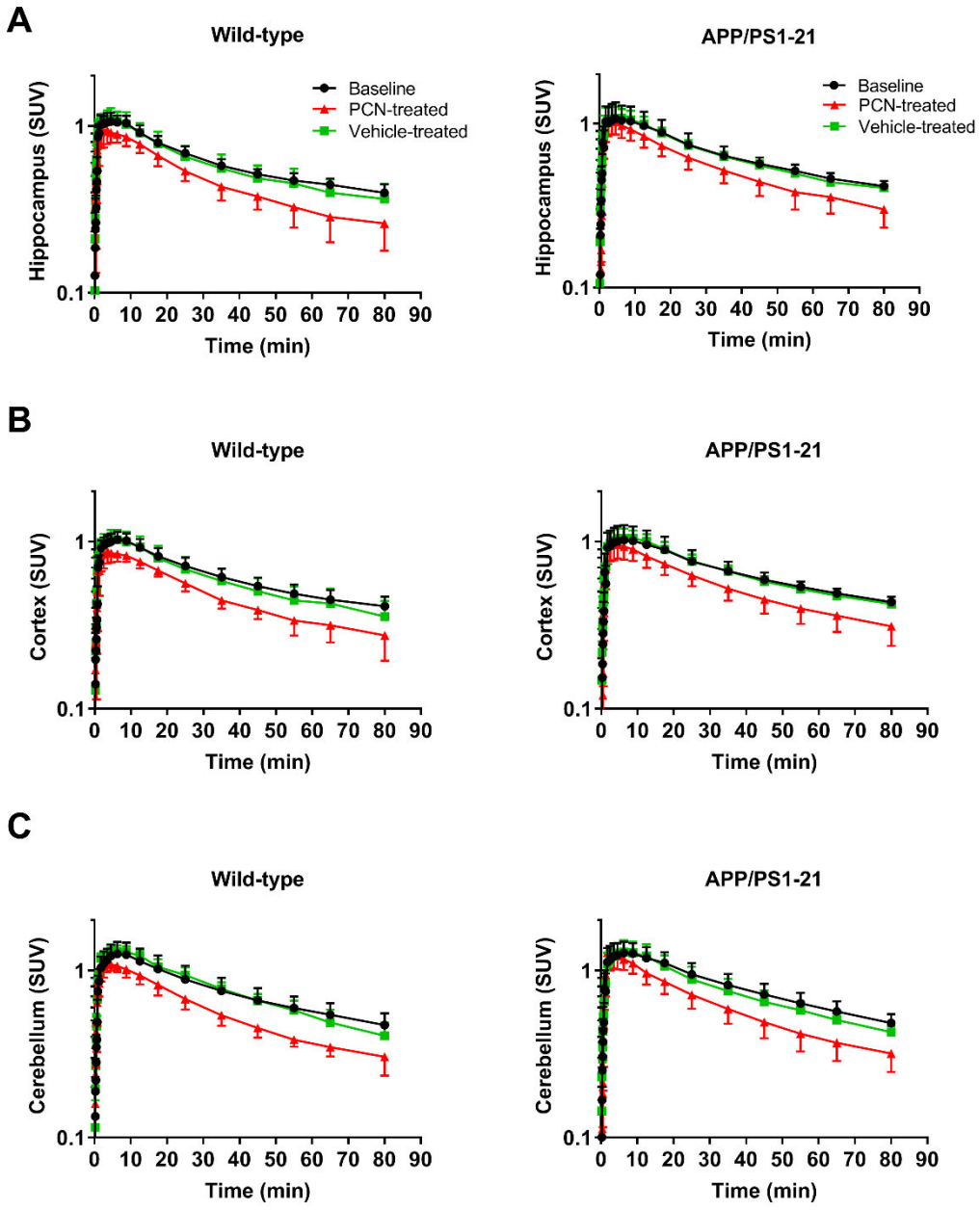

FIGURE 2. Mean (±SD) time-activity curves in wild-type mice and APP/PS1-21 mice aged 170 days for baseline PET scan and scan after i.p. treatment with PCN or vehicle for hippocampus (A), cortex (B) and cerebellum (C).

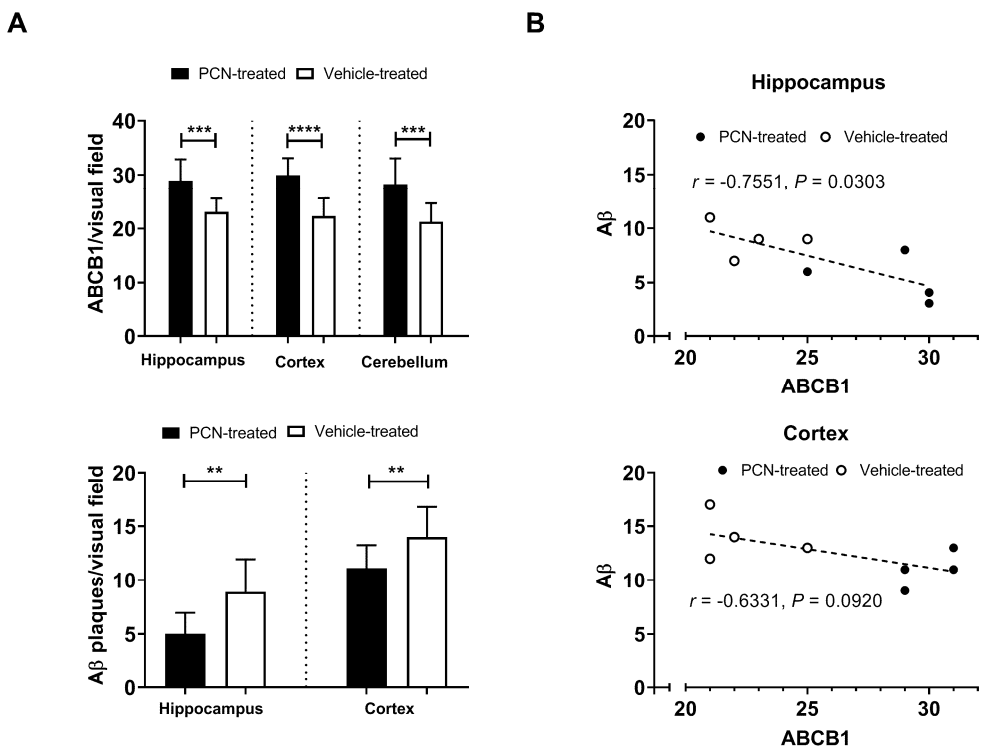

FIGURE 3. Semi-quantitative evaluation of stained ABCB1 in microvessels and Aβ plaques in the brains of APP/PS1-21 mice (A). Four visual fields (20x magnification) per mouse (n=4) were counted and the mean of each group was calculated. Error bars indicate standard deviation. Correlations between Aβ and ABCB1 in the hippocampus and in the cortex (B). Shown data are from APP/PS1-21 mice aged 170 days treated with PCN (filled circles, n=4) or vehicle (open circles, n=4). r=Pearson correlation coefficient. **, P<0.01, ***, P<0.001, ****, P<0.0001, 2-sided unpaired t-test

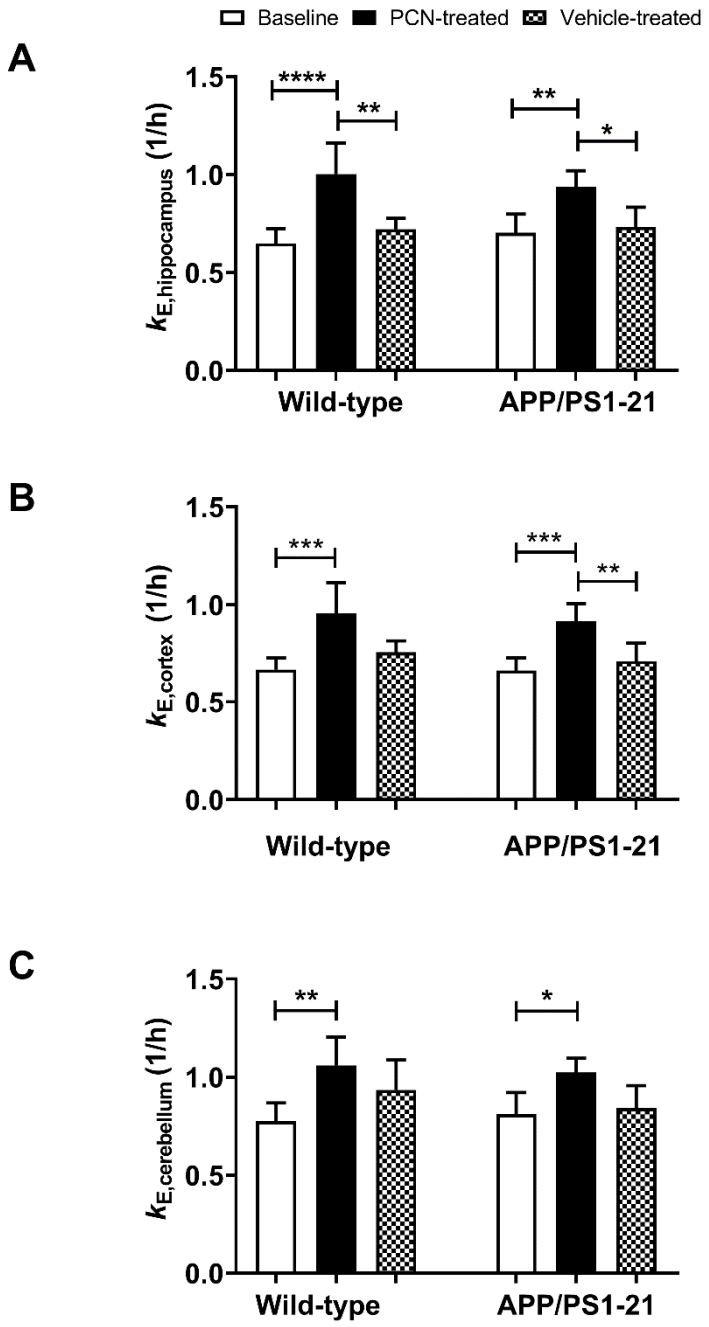

FIGURE 4. $k_{E,brain}$ values (mean±SD) for hippocampus (A), cortex (B) and cerebellum (C) in wild-type and APP/PS1-21 mice aged 170 days at baseline and after treatment with PCN or vehicle. *, P<0.05, **, P<0.01, ***, P<0.001, ****, P<0.0001, one-way ANOVA followed by Tukey's multiple comparison test

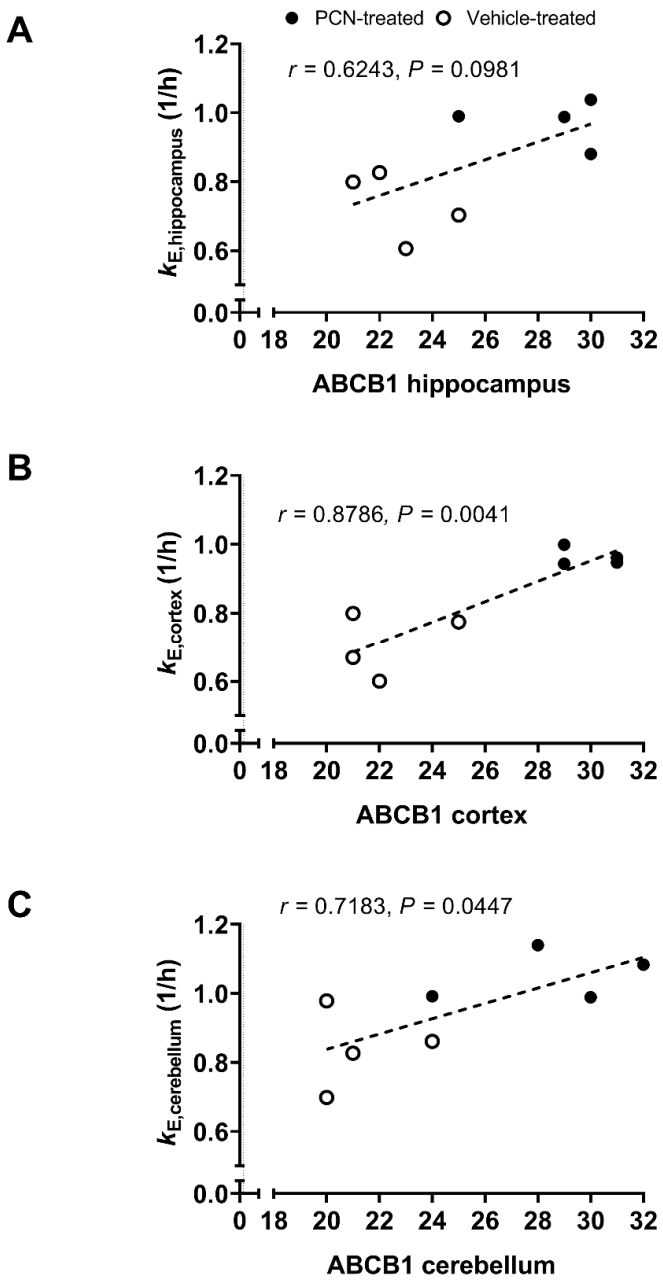

FIGURE 5. Correlations of $k_{E,brain}$ values with ABCB1 levels determined by immunohistochemistry in the hippocampus (A), cortex (B) and cerebellum (C) of APP/PS1-21 mice aged 170 days treated with PCN (filled circles, *n*=4) or vehicle (open circles, *n*=4). *r*=Pearson correlation coefficient

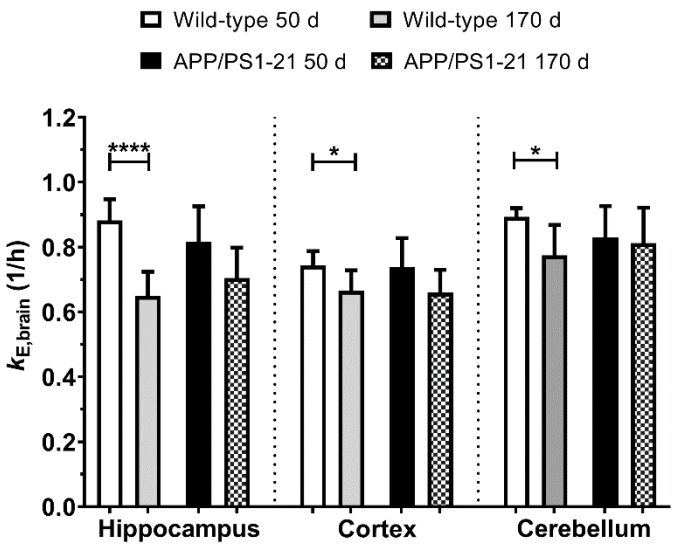

FIGURE 6. $k_{E,brain}$ values (mean±SD) for hippocampus, cortex and cerebellum of wild-type and APP/PS1-21 mice aged 50 and 170 days at baseline. *, $P<0.05$, ****, $P<0.0001$, 2-sided unpaired *t*-test

SUPPLEMENTAL DATA

SUPPLEMENTAL MATERIALS AND METHODS

Immunohistochemistry

Immunohistochemistry was carried out as described before (*1*). After defrosting from -80°C to -20°C, brains were cut in transversal 10 µm thick slices with a cryostat (Microm HM 550, Walldorf, Germany). Frozen sections of three brain regions including cortex, hippocampus and cerebellum were mounted on coated slides (VWR Superfrost Plus) and stored at -80°C. Later, the thawed brain slices were fixed either with 4% paraformaldehyde for ABCB1 staining or with methanol/acetone (1:1) for Aβ staining. After that, the slides were unmasked with acetic acid/ethanol (1:3) at -20°C for ABCB1 immunohistochemistry, washed in 0.1 M tris-buffered saline (TBS) and placed in endogenous peroxidase blocking solution consisting of 0.5% H_2O_2 (v/v) for 30 min. Afterwards, slides were washed and inserted into cover plates (Thermo Scientific™ Shandon™ Glass Coverplates, Fisher Scientific) to achieve standardized staining results. To avoid non-specific reactions, blocking solution was added for 1 h at room temperature. Brain slices were then incubated with the respective primary antibody (1:200, anti-P-glycoprotein antibody (EPR10364, recognizes both mouse ABCB1A and mouse ABCB1B), Abcam; 1:300, Anti-beta Amyloid antibody (ab3539), Abcam) or with antibody carrier solution for the negative control at 4°C overnight. On the next day, the slides were rinsed with TBS and the secondary antibody (1:500, Biotin-SP (long spacer) AffiniPure Donkey Anti-Rabbit IgG (H+L), Jackson Immuno Research) was applied at room temperature for 60 min. After three washing steps, antibody signals were amplified with the VectaStain ABC-Kit (Vector Laboratories) for 60 min at room temperature. After rinsing the slides with TBS, slides were incubated in nickel/diaminobenzidine solution for visualization of ABCB1 or Aβ. Slides were washed, dehydrated and mounted with Entellan®. For the semi-quantitative evaluation of ABCB1 in stained microvessels or Aβ plaques in the

hippocampus, cortex or cerebellum four visual fields (20x magnification) per mouse (*n*=4 animals per group) were counted and the mean of each group was calculated.

Metabolite Analysis

Female wild-type mice (*n*=4) and APP/PS1-21 mice (*n*=6) aged approximately 170 days were i.p. treated for 7 days once daily with either PCN (25 mg/kg) or its vehicle (5% dimethyl sulfoxide in safflower oil). One the day following the last treatment animals were i.v. injected *via* the tail vein under isoflurane/air anesthesia with ^{11}C-metoclopramide (15±12 MBq mixed with unlabeled metoclopramide, 2 mg/kg). After a period of 15 min, a terminal blood sample was collected from the retro-bulbar plexus and animals were killed by cervical dislocation while under deep anesthesia. Brain, liver, kidneys and gall bladder were removed and urine was collected. Blood was centrifuged to obtain plasma and proteins were precipitated by the addition of acetonitrile (1 µL per µL plasma). After homogenization of brain, liver and kidney tissue, acetonitrile was added to precipitate proteins (1000 µL per liver, 200 µL per brain/kidneys). Urine and bile were diluted by addition of acetonitrile (1 µL per 2 µL urine, 2 µL per µL bile). All solutions were vortexed and then centrifuged (12,000 g, 1 min, 21°C). Each supernatant (plasma, brain, liver, bile, kidneys, urine, 5 µL each) and diluted ^{11}C-metoclopramide solution as reference were spotted on thin-layer chromatography (TLC) plates (silica gel 60F 254 nm, 10 x 20 cm; Merck, Darmstadt, Germany) and plates were developed in ethyl acetate/ethanol/ammonium hydroxide (25%, w/v) (80/20/5, v/v/v). Detection was performed by placing the TLC plates on multisensitive phosphor screens (Perkin-Elmer Life Sciences, Waltham, MA). The screens were scanned at 300 dpi resolution using a PerkinElmer Cyclone® Plus Phosphor Imager (Perkin-Elmer Life Sciences). The retardation factor (R_f) for ^{11}C-metoclopramide was 0.45, while the radiolabeled metabolites remained on the start (R_f=0).

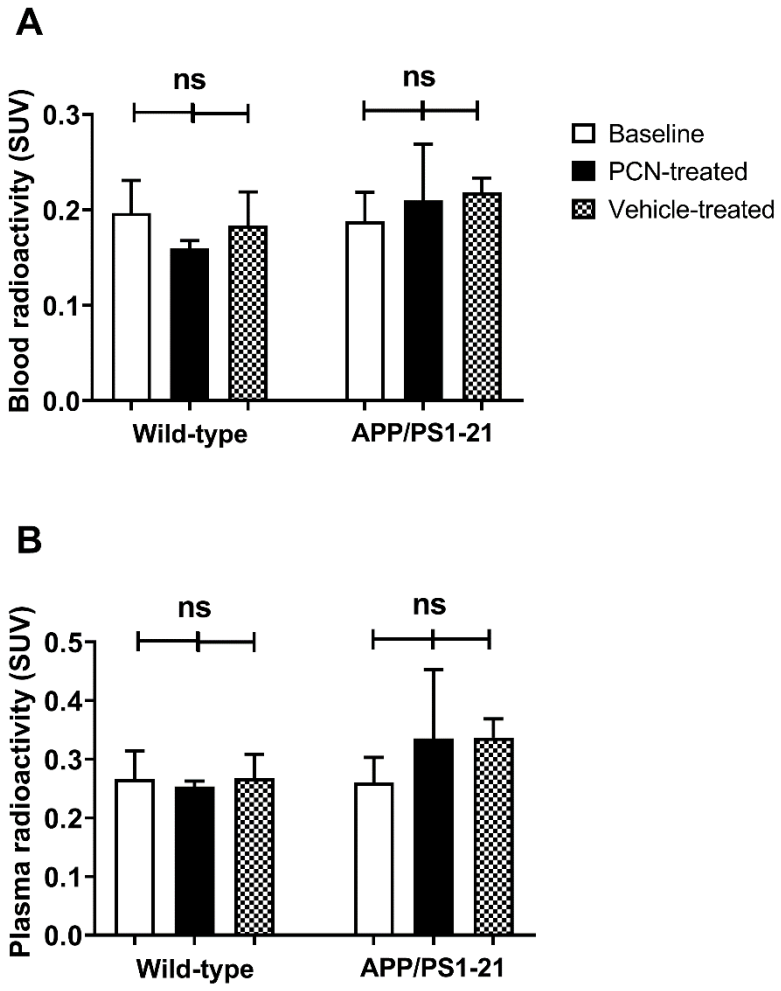

SUPPLEMENTAL FIGURE 1. Total radioactivity (mean±SD) in venous blood (A) and venous plasma (B) of samples collected at the end of the PET scan for wild-type and APP/PS1-21 mice aged 170 days at baseline and after treatment with PCN or vehicle. ns, not significant, one-way ANOVA followed by Tukey's multiple comparison test

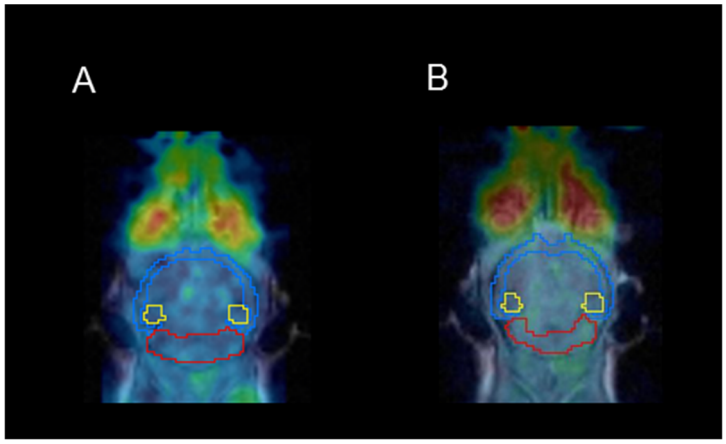

SUPPLEMENTAL FIGURE 2. Representative coronal MR co-registered PET summation images (0-90 min) in one wild-type mouse (A) aged 170 days and one APP/PS1-21 mouse (B) aged 170 days. The outlined regions of interest are shown: cortex (blue), hippocampus (yellow) and cerebellum (red). The cerebellum served as a control region without Aβ deposits (but with ABCB1 expression).

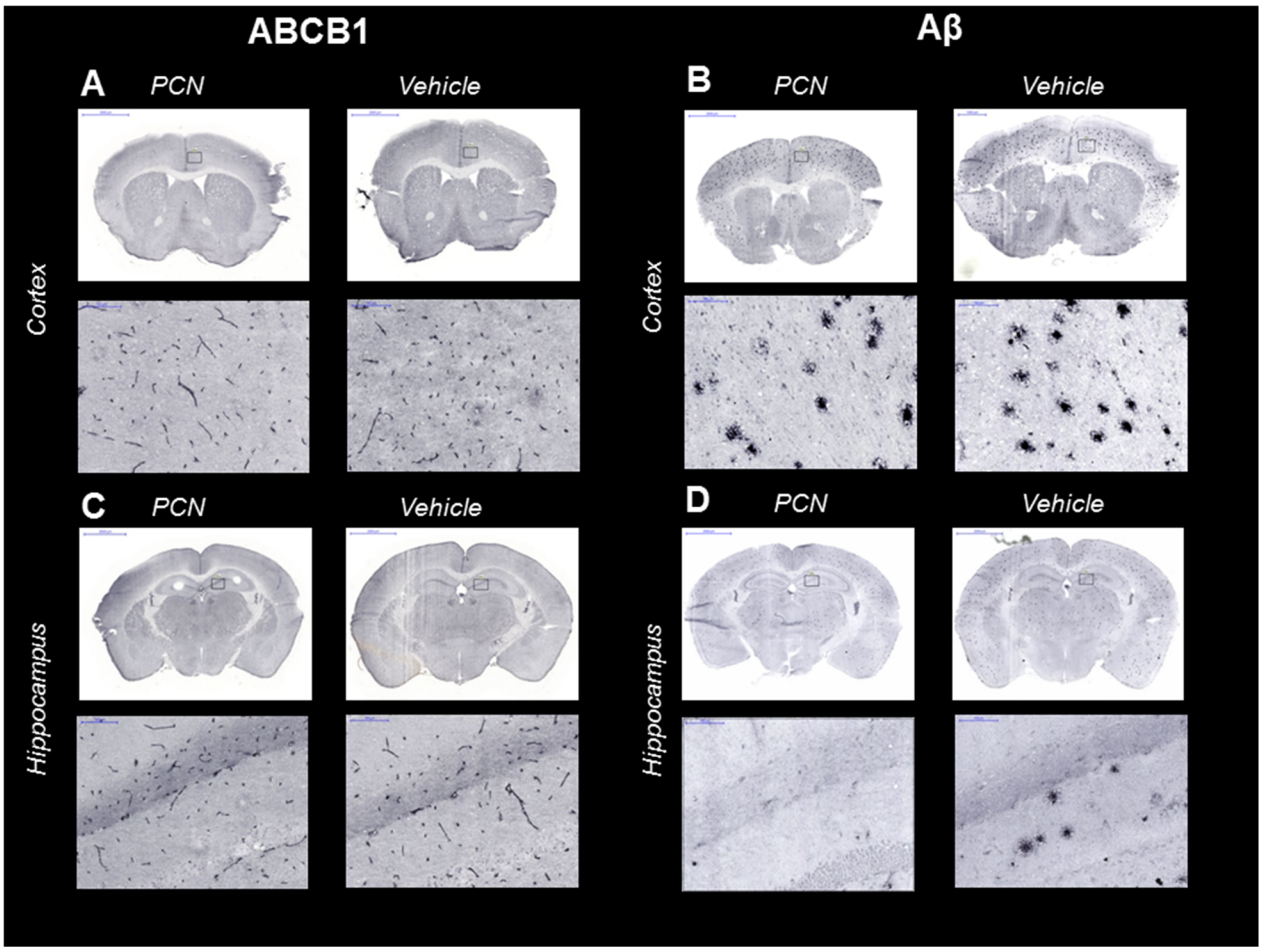

SUPPLEMENTAL FIGURE 3. Immunohistochemical staining of ABCB1 in brain microvessels (A, C) and Aβ (B, D) in the cortex and hippocampus of APP/PS1-21 mice aged 170 days treated with PCN or vehicle (scale bar=2000 µm). An enlarged section of the area is shown at a 20x magnification below each image (scale bar=100 µm).

SUPPLEMENTAL TABLE 1.

Metabolism of ^{11}C-Metoclopramide*

	Wild-type†	APP/PS1-21†	PCN-treated††
n	3	4	3
Plasma	39±8	24±2§	24±4§
Brain	92±4	82±7	86±7
Liver	78±3	61±3§	64±6§
Kidney	66±4	63±5	58±3
Bile	56±9	33±10	45±21
Urine	53±8	40±12	39±20

*Stated is the mean±SD percentage of unchanged ^{11}C-metoclopramide in different tissues and fluids determined with radio-thin-layer chromatography at 15 min after injection of ^{11}C-metoclopramide

†Animals were i.p. pretreated for 7 days once daily with PCN vehicle (5% dimethyl sulfoxide in safflower oil)

††Animals (wild-type: n=1, APP/PS1-21: n=2) were i.p. pretreated for 7 days once daily with PCN (25 mg/kg)

§P<0.05, for comparison with wild-type, one-way ANOVA followed by a Tukey's multiple comparison test

SUPPLEMENTAL TABLE 2

$k_{E,brain}$ Values in All Examined Animal Groups

Group	Region	$k_{E,brain}$ (1/h)
Wild-type baseline	Hippocampus	0.650±0.074
	Cortex	0.665±0.063
	Cerebellum	0.775±0.093
Wild-type PCN	Hippocampus	1.003±0.157
	Cortex	0.958±0.155
	Cerebellum	1.059±0.145
Wild-type vehicle	Hippocampus	0.722±0.055
	Cortex	0.758±0.059
	Cerebellum	0.934±0.152
APP/PS1-21 baseline	Hippocampus	0.704±0.094
	Cortex	0.660±0.070
	Cerebellum	0.812±0.109
APP/PS1-21 PCN	Hippocampus	0.938±0.083
	Cortex	0.918±0.089
	Cerebellum	1.023±0.073
APP/PS1-21 vehicle	Hippocampus	0.733±0.100
	Cortex	0.711±0.093
	Cerebellum	0.841±0.115
Wild-type baseline (50d)	Hippocampus	0.882±0.065
	Cortex	0.743±0.044
	Cerebellum	0.893±0.027
APP/PS1-21 baseline (50d)	Hippocampus	0.817±0.108
	Cortex	0.739±0.088
	Cerebellum	0.830±0.097

Values are reported as mean±standard deviation.
$k_{E,brain}$ (1/h), elimination slope for radioactivity washout from the brain

SUPPLEMENTAL REFERENCES

1. Zoufal V, Wanek T, Krohn M, et al. Age dependency of cerebral P-glycoprotein function in wild-type and APPPS1 mice measured with PET. *J Cereb Blood Flow Metab.* October 24, 2018 [Epub ahead of print].